

Cosmic Microwave Background Predictions of Supernatural Inflation

by
Catalina M. Buttz

Submitted to the Department of Physics
in partial fulfillment of the requirements for the degree of
Bachelor of Science in Physics
at the

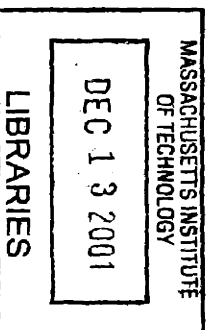
MASSACHUSETTS INSTITUTE OF TECHNOLOGY
[June 2001]
August 2001

© Massachusetts Institute of Technology 2001. All rights reserved.

Author
Department of Physics
August 21, 2001

Certified by
Alan H. Guth
Victor F. Weisskopf Professor of Physics
Thesis Supervisor

Accepted by
David Pritchard
Senior Thesis Coordinator



ARCHIVES

Cosmic Microwave Background Predictions of Supernatural Inflation

by

Catalina M. Buttz

Submitted to the Department of Physics
on August 21, 2001, in partial fulfillment of the
requirements for the degree of
Bachelor of Science in Physics

Abstract

This thesis makes predictions for the temperature anisotropy spectrum of the CMB under the supernatural inflation model class [17] and compares these predictions against the Boomerang 98 data [5], using the Lange *et al* [11] cosmological parameter estimations for an $\Omega_{tot} = 1$ universe. This was implemented by creating a modified version of CMBFAST [19] which could accommodate a two-field inflation model. A series of codes were compiled, both with and without modifications, to determine the effect of the supernatural primordial spectrum spike on CMB simulations at the Planck, GUT and Intermediate energy scales, where the inflaton field has renormalizable couplings to other fields. While the spike's effects at $1Mpc$ were found to be negligible, the detailed calculations of the scalar spectral index, n_s , demonstrate that the energy scale most favored by Randall *et al* on particle physics grounds, is actually the one most tightly constrained by observation.

Thesis Supervisor: Alan H. Guth

Title: Victor F. Weisskopf Professor of Physics

Acknowledgments

To properly thank all the people who made this work possible would require a volume independent of this one, so I heartily apologise for leaving anyone out! I first and foremost thank my advisor, teacher, and friend, Professor Alan H. Guth for his patience, guidance and encouragement. Dr. Robert Lopez was instrumental in providing instruction for the computational portions of this work and was great fun to work with. I would also like to thank Peggy Berkowitz, MIT UROP, the staff at the MIT Physics Education Office, the staff at Cambridge University's Isaac Newton Institute for the Mathematical Sciences, Senior Tutor Dr. Paul Beattie at Corpus Christi College, Cambridge University and Dr. Matias Zaldarriaga, the author and consultant of CMBFAST for providing the resources for this research. The support of my family and friends during my time at MIT and Cambridge was indispensable. In particular, Diana, Gabriela, Angelina, Donald Buttz as well as Christopher J. Hardgrove, Lita H. Lee, Jason E. Martinez, Kristin Burgess, Dr. Peter Reich, Dean Arnold Henderson, Phillip Bernard, Joji, Robert Weinerman, Professor Jeffrey Goldstone, Professor Paul Schechter, Professor Krishna Rajagopal, Anna Doney-Zeffertt, Alex Zeffertt, Stafford Lowe, Tania King, and Dominic Latter were incredibly supportive. Professor Alan Guth, Jeffrey Bowers and Dimitri Kountourgiannis provided many useful comments on their reviews of the manuscript and were particularly helpful during the final stages of this project. Finally, I'd like to thank Perry Bamonte for his genuine interest in cosmology and astrophysics that reminded me during some of the most difficult stages of this project why I undertook it in the first place.

This work was supported by MIT-NASA Space Grant Consortium, MIT UROP, Dr. Angelina I. Buttz, Gabriela I. Buttz, and Diana C. Buttz.

Contents

1	Introduction	10
2	Supernatural Inflation	15
2.1	Motivations for supersymmetry	16
2.2	Tree-level potential	17
2.3	General relativity and the action principle	18
2.4	Equations of motion for the scalar fields	20
2.5	Supernatural inflation potential function	22
2.6	Dynamics of the scalar fields	24
3	CMB Anisotropy Formation	32
3.1	Overview	32
3.2	Cosmological perturbations	35
3.3	Multipoles	36
4	CMB Temperature spectrum computation	39
4.1	CMBFAST and modifications	39
4.2	Checking the magnitude of fluctuations	40
4.3	Calculating the CMB spectrum	42
4.4	Discussion	45

List of Figures

1-1	This figure [21] summarizes the current experimental results as of June 2000. The red curve is Tegmark's best-fit to the data.	11
1-2	This figure summarizes the angular sensitivity of CMB experiments, and is from [22]. The shaded regions indicate where the various foregrounds cause fluctuations exceeding those of COBE-normalized scale-invariant fluctuations, thus posing a substantial challenge to estimation of genuine CMB fluctuations. They correspond to dust (red), free-free emission (cyan), synchrotron radiation (magenta), and point sources (green). The heavy dashed lines show the frequency where the total foreground contribution to each multipole is minimal. The boxes indicate roughly the range of multipoles ℓ and frequencies ν probed by various CMB experiments.	12
2-1	<i>"Sir Isaac Newton wore his black and gold waistcoat." - The Tale of Jeremy Fisher - Beatrix Potter</i>	15
2-2	Graphical representation of a supernatural inflation potential.	24
2-3	Parameter choices for supernatural inflation with M' at the Planck scale. Here μ_ϕ is chosen to give the correct magnitude of density fluctuations for the minimum μ_ϕ consistent with a sufficiently rapid end to inflation.	30
2-4	Parameters for supernatural inflation with M' at the GUT scale. The values were chosen by the same criteria used in figure (2-3).	30

2-5	Parameters for supernatural inflation with M' at the intermediate scale. The values were chosen by the same criteria used in figure (2-3).	31
3-1	This figure is a preliminary map of a collaborative effort (involving A.J. Bandy, K.M. Górski, G. Hinshaw and A. Kogut) to remake COBE-DMR four year sky maps in the Healpix format [6] (see also http://www.tac.dk/healpix/skymaps1.html). This map is shown in Galactic coordinates, and was made at a higher resolution than the previously released public maps smoothed to an effective beam resolution of 10 degrees. It is shown in mK .	34
4-1	The magnitude of the spike generated by the ϕ field in supernatural inflation. The horizontal line represents the Peebles-Harrison-Zeldovich spectrum characteristic of COBE data.	41

4-2 Angular power spectrum measured by Boomerang at 150 GHz, taken from [5]. Each point is the power averaged over $\Delta\ell = 50$ and has negligible correlations with the adjacent points. The error bars indicate the uncertainty due to noise and cosmic/sampling variance. The errors are dominated by cosmic/sampling variance at $\ell < 350$; they grow at large ℓ due to the signal attenuation caused by the combined effects[3] of the 10' beam and the 14' pixelation (0.87 at $\ell = 200$ and 0.33 at $\ell = 600$). The current $\pm 10\%$ uncertainty in the calibration corresponds to an overall re-scaling of the y -axis by $\pm 20\%$, and is not shown. The current 1' uncertainty in the angular resolution of the measurement creates an additional uncertainty—indicated by the distance between the ends of the red error bars and the blue horizontal lines—that is completely correlated and is largest (11%) at $\ell = 600$. The green points show the power spectrum of a difference map obtained as follows: the data was divided into two parts, corresponding to the first and second halves of the time stream. Two maps (A and B) were made from these halves, and the green points show the power spectrum computed from the difference map, $(A - B/2)$. Signals originating from the sky should appear in this map, so this is a test for data contamination. The solid curve has parameters ($\Omega_b = 0.05$, $\Omega_m = 0.31$, $\Omega_\Lambda = 0.75$, $n_s = 0.95$, $h = 0.70$), and is the best model fit for the Boomerang test flight data [14, 15], and is shown for comparison only. 43

4-3 In all the curves which appear above, the following cosmological parameters were used: ($\Omega_{tot} = 1, \Omega_b = 0.04, \Omega_c = 0.26, \Omega_\Lambda = 0.04, \tau_c = 0.025, T_0 = 2.728K, Y_{He} = 0.24$). The top curve is the CMB temperature anisotropy spectrum for supernatural inflation at the intermediate scale using either the CMBFAST default $\mathcal{P}_{\mathcal{R}}(k)$ with $n_s = 1.0332, \mathcal{P}_{\mathcal{R},\psi}(k)$, or $\mathcal{P}_{\mathcal{R}modified}(k)$. The middle curve was calculated in the same way for supernatural inflation at the GUT or Planck scales, with $n_s = 1.00$. The bottom curve is a reproduction of the the Lange, *et. al*/P11 curve, [11]. 45

List of Tables

4.1	Energy Scales of Peak Parameters in Supernatural Inflation	42
4.2	This table is a sample of some results of parameter extraction using the method of successfully more restrictive priors. The confidence intervals are 1σ . The 2σ values are approximately double the 1σ values quoted in most cases; upper limits are quoted at 2σ . The quoted values are reported after marginalizing over all other parameters. The weak h priors are tophat functions (uniform priors) and include an additional age $> 10Gyr$ prior. The LSS priors are combinations of Gaussians and tophats. Columns 1-5 (Ω_{tot} to Ω_Λ) are predominantly driven by the CMB data, except for $\Omega_b h^2$ and Ω_b when the strong BBN prior is applied. Most of the parameters in columns 6-10 (τ_c to Age) are influenced by the structure of the parameter space and should not be interpreted as CMB-driven constraints; exceptions are the $\Omega_c h^2$ and Ω_Λ results when the LSS prior is applied.	44

Chapter 1

Introduction

“It is with humility really unassumed – it is with a sentiment even of awe – that I pen the opening sentence of this work: for of all conceivable subjects I approach the reader with the most solemn – the most comprehensive – the most difficult – the most august.”

- Eureka: An essay on the material and spiritual universe. – Edgar Allan Poe

Among the relics of the early universe available to observers, anisotropies in the cosmic microwave background are robust to model changes, and enable cosmologists to probe the universe back to redshifts of order $z \approx 1000$. In addition, both the physics and equations to be solved in studying the CMB are theoretically relatively elementary. All that is required is relativistic kinetic and perturbation theory to describe the evolution of the cosmic microwave background anisotropies.

Not only are the equations involved elementary, a linear approximation is well justified since the anisotropies in the microwave background were produced when the universe was almost perfectly homogeneous. This linearity distinguishes CMB anisotropies from other more local probes such as galactic surveys because non-linearity complicates the theoretical interpretation of the data in those experiments.

There is a wealth of information encoded in the CMB radiation field. Indeed, the flood of data from COBE and other CMB experiments (see figure 1-1) in the last ten

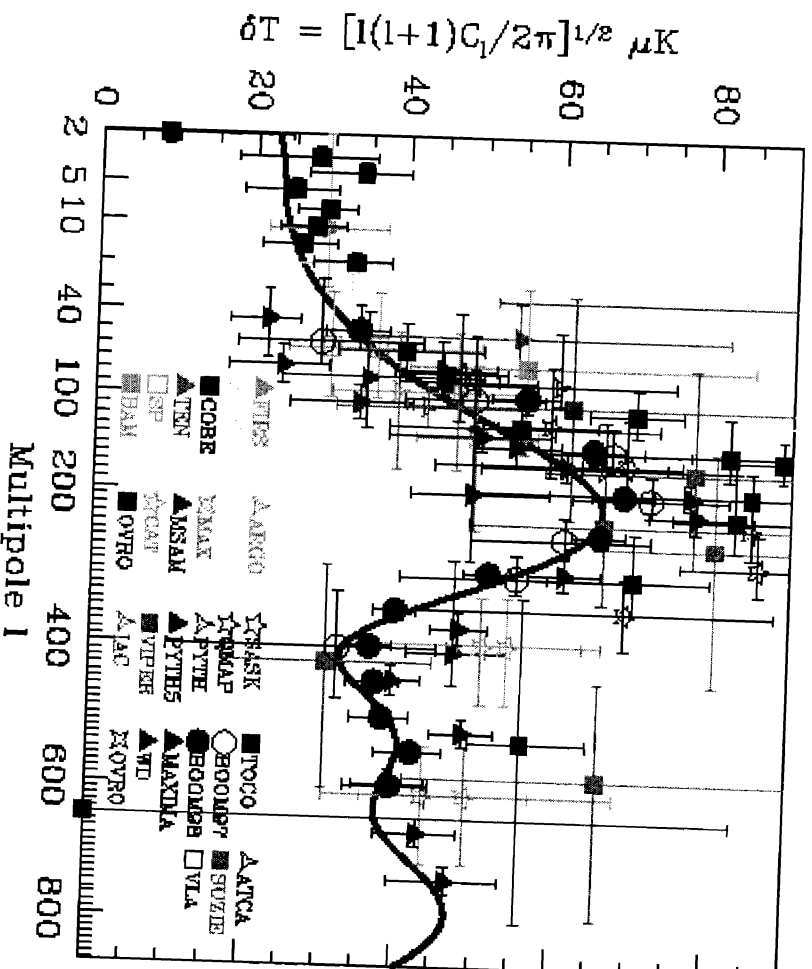


Figure 1-1: This figure [21] summarizes the current experimental results as of June 2000. The red curve is Tegmark's best-fit to the data.

years has moved cosmology from armchair philosophy to precision science, and has the potential of dramatically changing our understanding of the universe. In the last decade the COBE[20] satellite provided definitive evidence that the universe began in a hot big bang and that it is homogeneous and isotropic on large scales. In the next decade the age, size and fate of the universe might be just as definitive.

The most promising solution for these questions thus far is the inflationary paradigm, the most general feature of which is that the universe began with a state of accelerated expansion. Indeed, since Guth's seminal paper of 1981 [7], there have been many types of inflationary models introduced, motivated by developments in particle theory and in anticipation of what future observations might bring.

One such inflationary scenario is Randall *et al.*'s [17] supernatural inflation. This class of models uses weak scale supersymmetry breaking to construct inflationary

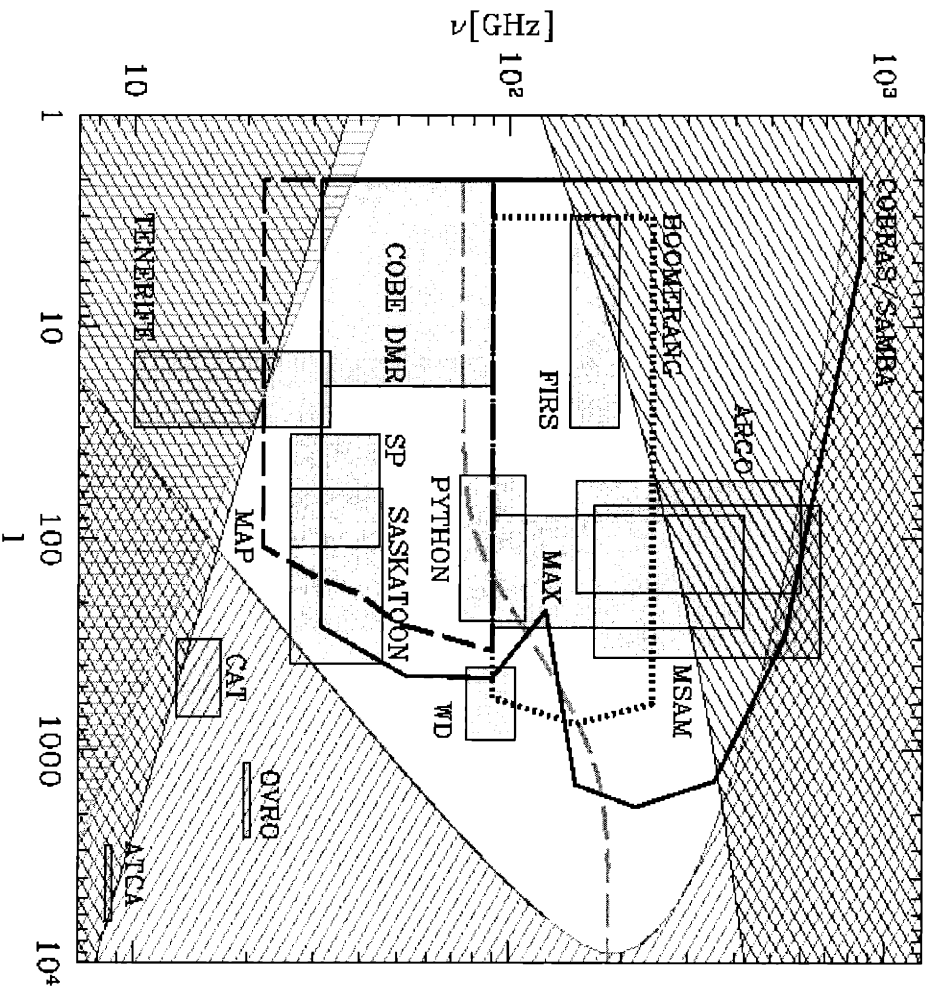


Figure 1-2: This figure summarizes the angular sensitivity of CMB experiments, and is from [22]. The shaded regions indicate where the various foregrounds cause fluctuations exceeding those of COBE-normalized scale-invariant fluctuations, thus posing a substantial challenge to estimation of genuine CMB fluctuations. They correspond to dust (red), free-free emission (cyan), synchrotron radiation (magenta), and point sources (green). The heavy dashed lines show the frequency range where the total foreground contribution to each multipole is minimal. The boxes indicate roughly the range of multipoles ℓ and frequencies ν probed by various CMB experiments.

models with parameters that appear naturally as mass ratios of supersymmetric particles. This is an unusual feature since most inflationary models contain one or more unmotivated small parameters.

Structure formation in inflationary cosmologies typically leaves between five and twelve parameters to be fixed by comparison to the observational data, namely,

Inflationary parameters: $\delta_H, n_s, \tau, n_T, dn/d\ln k \dots$

Cosmological parameters: $H_0, \Omega_b, \Omega_0, \Omega_\Lambda, \Omega_{HDM}, g_*, \kappa, Y_{He}, T_{CMB} \dots$

Of course, cosmologists would be very unlucky indeed if all these parameters were relevant. In the inflationary picture, as an absolute minimum, one would consider a power-law spectrum of density perturbations parametrized by a normalization factor and the spectral index, n_s . The general result would also include gravity waves, thereby introducing τ , the ratio of tensor to scalar perturbations. The tensor spectral index, n_T is related to τ by a consistency relation. Any deviations from power-law approximation can be examined by considering derivatives such as $dn/d\ln k$, and in fact, this would be extremely interesting for inflation if these are significant since they would provide information about the potential energy of the scalar field that drives inflation.

The predictions for these parameters under supernatural inflation are a very low Hubble constant during inflation, on the order of $10^3 - 10^4 GeV$, a scalar density perturbation index $n_s \approx 1$, negligible tensor perturbations, and a novel large spike in the density perturbation spectrum at short wavelengths. While the amplitude of the power-law spectrum of most inflationary models is usually adjusted to fit the data, the spike found in supernatural models arises from supersymmetric particle physics which allows little freedom in adjusting its amplitude.

On the cosmological side the Hubble constant H_0 and Ω_b , the baryon density, must be considered as a minimum since the temperature power spectrum is very sensitive to both. If polarization is measured, then κ , the optical depth to the surface of last

scattering (or, equivalently, the reionization redshift, z_{ion}), must also be considered since the polarization power spectrum is quite sensitive to it. The parameter, g_* , represents the number of relativistic species. This determines the epoch of matter-radiation equality and can be calculated using the particle physics model under which the inflation scenario is based. The remaining parameters could be fixed by assumption, for example, a critical density, cold dark matter universe. It should be noted that in a scenario with significant reionization, it may be necessary to model it in a more sophisticated manner than just as a single redshift of instantaneous reionization.

The crucial role of CMB experiments (see figure 1-2) as far as inflationary cosmology is concerned is parameter estimation. On mid- to small- angular scales the predicted temperature power spectrum curve depends on a large number of parameters and contains sufficient structure to allow many of them to be determined to unprecedented accuracy. Theoretical predictions for the temperature and polarization power spectrum curves can be made using the publicly available code CMBFAST, which can predict the temperature power spectrum to an accuracy of 1 percent.

This thesis makes predictions for the temperature anisotropy spectrum of the CMB under the supernatural inflation model and compares these predictions against experimental CMB data. Chapter 2 begins with a discussion of supernatural inflation. This is followed by a description of CMB anisotropy formation in Chapter 3. Chapter 4 presents a brief overview of CMBFAST the publicly available Boltzmann code, and the modifications made to produce a plot of the CMB temperature anisotropy spectrum under supernatural inflation.

Chapter 2

Supernatural Inflation



Figure 2-1: “*Sir Isaac Newton wore his black and gold waistcoat.*” - *The Tale of Jeremy Fisher* – *Beatrix Potter*

All the standard models of inflation are based on a type of matter known as a scalar field. Particle physics has not yet offered a definitive view on the detailed properties of these fields and in particular has not specified the potential energy which, as it turns out, is responsible for driving the inflationary expansion. Thus the freedom exists to build a wide range of inflationary models based on different choices of the potential energy and perhaps different motivations for its particle physics origin. At its most minimal a model of inflation simply gives the form of the effective potential, V_{eff} during inflation, and a description of how inflation will end. However, it is also desirable that inflation be sensible with particle physics, such that in the end it

will belong to a complete theory that describes all of the particles and interactions occurring in Nature.

2.1 Motivations for supersymmetry

Supersymmetry in some form is often thought to be inevitable because of the gauge hierarchy problem, which asks how can it be that the real world exists so far below the GUT scale, *i.e.* why is $\frac{M_W}{M_{GUT}} \approx 10^{-13}$? Such a number is unnatural because quantum corrections would be expected to perturb the bare value of the W mass by a significant fraction of the GUT scale. In the absence of any other idea for sustaining the gauge hierarchy, supersymmetry has been taken as a very real possibility in particle physics.

The full mathematical implementation of supersymmetry (SUSY) is quite technical [2]. Thus only the key points relevant to supernatural inflation are highlighted here. Without SUSY quantum effects generally give each fundamental scalar field a mass on the order of the Planck mass, M_p , and a delicate cancellation is required in order to obtain sensible masses. However, SUSY provides a means for quantum corrections to be automatically cancelled. Each known particle must have a superpartner: boson A implies the fermion A-ino and fermion B implies the boson s-B, populating the universe with a number of fundamental scalar fields not introduced in the standard model. In addition in a supersymmetric theory these scalar fields are complex because they are partners of left or right-handed fermionic fields with two components. Finally, it is expected to be a local symmetry.

Unbroken SUSY would require that each particle has the same mass as its superpartner. Since this is not observed SUSY must be broken in the present vacuum. This is presumably achieved through the spontaneous breaking of supergravity, which at low energies looks like the explicit breaking of global SUSY through certain so-called soft SUSY breaking terms in the Lagrangian. In the early universe additional SUSY breaking occurs and during inflation it typically dominates soft SUSY breaking if $V^{\frac{1}{4}} \geq M_S$ where the scale M_S depends on the mechanism of SUSY breaking. Scales of interest in supersymmetric field theories include the Planck scale, $M_p \approx 10^{19} GeV$,

the GUT scale $M_G \approx 10^{16} GeV$, the intermediate scale, $M_I \approx 10^{11} GeV$ and the supersymmetry breaking scale, $m_{3/2} \approx 1 TeV$.

2.2 Tree-level potential

In quantum field theory, the effective potential in the perturbative regime is given by the sum of Feynman diagrams. They can be classified by the number of loops present in the diagram. The no-loop, or tree-level diagram is roughly speaking, the classical object that appears in the Lagrangian, and in some simple cases the tree-level potential is a good approximation to the exact solution. The potential is constructed out of powers of the fields present and in the context of supergravity, there will be an infinite number of terms.

However, supergravity corrections tend to generate a steep potential that is unable to sustain single-field inflation. This consideration, among others, has led to the development of a class of models known generically as hybrid inflation. These models rely on interactions between two scalar fields, and utilize the flat potentials expected in supersymmetric theories. Multiple field, or hybrid inflation models can give substantial inflation for a much more modest evolution of the scalar field, remaining always much less than the Planck mass; a more detailed discussion will be made in the context of supernatural inflation.

A strong criticism of most inflationary models is that they use unmotivated small parameters in the particle theory Lagrangian to provide the flat potential required for sufficient inflation and to result in density fluctuations with magnitudes within experimental bounds. Models in which these parameters are ratios of known particle physics mass scales have been suggested as a solution to this problem [1].

2.3 General relativity and the action principle

As far as we know, the properties of any system in fundamental physics can be specified by its action,

$$S = \int_{-\infty}^{\infty} L dt. \quad (2.1)$$

To have a Lorentz-invariant action, the Lagrangian for the fields must be of the form $L = \int \sqrt{-g} \mathcal{L} d^3\tau$, where the Lagrangian density \mathcal{L} is Lorentz-invariant and has dimensions [energy]⁴. It is a function of the fields and their first derivatives with respect to space and time. Higher derivatives would not lead to sensible physics. In what follows we consider only scalar fields since they are what is needed for inflation and the main effect of other fields, as far as inflation is concerned, is likely to be in the loop correction mentioned earlier.

Because the volume element in generic coordinates is $d^4x \sqrt{-g}$, the action of a system will be of the form

$$S = \int d^4x \sqrt{-g} \mathcal{L}. \quad (2.2)$$

By making a small variation, $\delta g_{\mu\nu}$, whose first derivatives vanish at infinity, the action principle, $\delta S = 0$ yields the Einstein equation. The most general possibility leading to the Einstein equation is the Einstein-Hilbert Lagrangian density,

$$\mathcal{L} = \frac{1}{16\pi G} R + \mathcal{L}_{matter}. \quad (2.3)$$

The first term is the Einstein Lagrangian and represents the Lagrangian for gravitation. The space-time curvature, R , is to be regarded as a function of $g_{\mu\nu}$ and its first space-time derivatives. To obtain the full field equations, it must be assumed that there are other fields beside the gravitational field, which can be described by the second term, the matter Lagrangian.

Varying $g_{\mu\nu}$ in the action principle gives the Einstein equation (see [16]) with,

$$T_{\mu\nu} = -2 \frac{\partial \mathcal{L}_{matter}}{\partial g^{\mu\nu}} + g_{\mu\nu} \mathcal{L}_{matter}. \quad (2.4)$$

Note that it should be expected that the matter Lagrangian involves only the first derivative of $g_{\mu\nu}$ because \mathcal{L}_{matter} is to be identified with the special-relativistic Lagrangian density, which describes fields in the absence of gravity. In going from a special-relativistic to a general-relativistic expression, $\eta_{\mu\nu}$ would be replaced by $g_{\mu\nu}$, and ∂_μ by D_μ . In general D_μ contains only $g_{\mu\nu}$ and its first derivative. But when D_μ acts on a scalar field, the first derivatives do not appear, and D_μ is just ∂_μ .

In the case of a hybrid inflation model like supernatural inflation, there are two scalar fields, which contribute to \mathcal{L}_{matter} . The mandatory complex scalar fields of supersymmetry correspond to a pair of real fields, which are the relevant fields for inflation. Thus, a pair of complex scalar fields, Ψ and Φ can be written as $\Psi \equiv \frac{1}{\sqrt{2}}(\psi + i\psi_i)$ and similarly for Φ .

The Lagrangian density for the real parts of these scalar fields in a generic coordinate system is given by,

$$\mathcal{L}_{matter} = -\frac{1}{2}g^{\mu\nu}\partial_\nu\psi\partial_\mu\psi - \frac{1}{2}g^{\mu\nu}\partial_\nu\phi\partial_\mu\phi - V(\psi, \phi). \quad (2.5)$$

The stress-energy tensor for two scalar fields is therefore

$$T_{\mu\nu} = \partial_\nu\psi\partial_\mu\psi + \partial_\nu\phi\partial_\mu\phi - g_{\mu\nu}\left[\frac{1}{2}g^{\alpha\beta}\partial_\alpha\psi\partial_\beta\psi + \frac{1}{2}g^{\alpha\beta}\partial_\alpha\phi\partial_\beta\phi + V(\psi, \phi)\right]. \quad (2.6)$$

Using this equation and by following the above prescription for varying the action, the Einstein field equation for this system is,

$$R_{\mu\nu} - \frac{1}{2}g_{\mu\nu}R + \Lambda g_{\mu\nu} = 8\pi GT_{\mu\nu} \quad (2.7)$$

where $R_{\mu\nu}$ is the Ricci tensor, $g_{\mu\nu}$ is the metric, R the curvature scalar, Λ is the cosmological constant, G is Newton's gravitational constant.

By asserting that the right hand side of the above equation is the source of gravity, and taking the energy-momentum tensor to be a smoothly varying function of position, relativistic fluid flow is effectively being described using $T^{\mu\nu}$. To simplify the analysis, consider the limit of flat space-time, where G tends to zero, but this

definition of $T^{\mu\nu}$ still holds. At any point in space-time, the local rest frame of the fluid is defined as the frame in which the momentum density, T^{0i} , vanishes, the energy density is defined as $\rho = T^{00}$, and the stress tensor is $T_{ij} = T_{ji}$. If the stress is isotropic, the pressure P by $T_{ij} = \delta_{ij}P$. Assuming the stress is indeed isotropic, the energy density and pressure for this system are given by,

$$\begin{aligned}\rho &= \frac{1}{2}(\dot{\psi}^2 + \dot{\phi}^2) + V(\psi, \phi) \\ P &= \frac{1}{2}(\dot{\psi}^2 + \dot{\phi}^2) - V(\psi, \phi)\end{aligned}$$

Note that although these scalar fields act as a perfect fluid, they do not possess an equation of state relating ρ and P because the same energy density can correspond to different values of the pressure if the energy density is distributed differently between the potential and kinetic terms.

By inserting the Robertson-Walker metric describing a homogeneous and isotropic universe into the Einstein field equations, the time derivative of the Friedmann equation (c.f. Carroll, Press, Turner, Peacock) gives the acceleration equation,

$$\frac{\ddot{a}}{a} = -\frac{4\pi G}{3}(\rho + 3P) + \frac{\Lambda}{3} \quad (2.8)$$

where the function, $a(t)$, is a universal scale factor and t is cosmic time. The precise definition of inflation is simply an epoch during which the scale factor of the universe is accelerating, *i.e.*, $\ddot{a} > 0$. Directly from the acceleration equation above, with $\Lambda = 0$, or absorbed into ρ and P , the condition for a two-field hybrid inflation model like supernatural inflation can also be written as,

$$\rho + 3P = 2(\dot{\psi}^2 + \dot{\phi}^2) - \frac{1}{2}V(\psi, \phi) < 0. \quad (2.9)$$

2.4 Equations of motion for the scalar fields

While making a small variation in $\delta g_{\mu\nu}$ using the action principle $\delta S = 0$ gives the Einstein equation, making small variations in the fields ψ and ϕ using the action

principle gives rise to the scalar wave equations for ψ and ϕ .

Using the flat R-W metric,

$$ds^2 = -dt^2 + a^2(t)d\vec{x}^2 \quad (2.10)$$

the action,

$$S = \int d^4x \sqrt{-g} \mathcal{L} \quad (2.11)$$

can be written as

$$S = \int d^4x \tilde{\mathcal{L}} \quad (2.12)$$

where $\tilde{\mathcal{L}} = a^3(t)\mathcal{L}$. Varying the action with $\delta\partial_\mu\psi = \partial_\mu\delta\psi$ and assuming $\delta\psi = 0$ at the boundary gives,

$$\delta S = \int d^4x \left\{ \frac{\partial \tilde{\mathcal{L}}}{\partial \psi} \delta\phi + \frac{\partial \tilde{\mathcal{L}}}{\partial (\partial_\mu \psi)} \delta(\partial_\mu \psi) \right\}. \quad (2.13)$$

Integrating by parts the above expression gives,

$$\delta S = \int d^4x \left\{ \frac{\partial \tilde{\mathcal{L}}}{\partial \psi} - \partial_\mu \left(\frac{\partial \tilde{\mathcal{L}}}{\partial (\partial_\mu \psi)} \right) \right\} \delta\psi(x) = 0. \quad (2.14)$$

By requiring that $\delta S = 0$ ¹, the equation of motion for the ψ field is given by,

$$\ddot{\psi} + 3H\dot{\psi} - \frac{\partial V}{\partial \psi} = 0. \quad (2.15)$$

It follows exactly similarly for the ϕ field,

$$\ddot{\phi} + 3H\dot{\phi} - \frac{\partial V}{\partial \phi} = 0. \quad (2.16)$$

Using the Friedmann equations,

$$H^2 = \frac{1}{3M_p^2} \left[V(\psi, \phi) + \frac{1}{2}\dot{\psi}^2 + \frac{1}{2}\dot{\phi}^2 \right],$$

¹Note that the comoving volume in an inflating universe is given by $a^3 = e^{3Ht}$. The Hubble parameter, $H = \dot{a}/a$

the scalar wave equations and the forms of the effective energy density and pressure, the condition for inflation is satisfied provided that $\frac{1}{2}\dot{\psi}^2 + \frac{1}{2}\dot{\phi}^2 < V(\psi, \phi)$. With a suitably flat potential, even if this condition is not satisfied initially, it very quickly comes to be obeyed, provided that the scalar field is displaced away from the minimum of its potential. Note also that once inflation gets underway the curvature terms in the Friedmann equations are rendered less and less important.

In fact these terms are normally taken to be negligible from the start, and since the $\ddot{\psi}$ and $\ddot{\phi}$ terms are of the same order, ignoring them gives,

$$H^2 \approx \frac{V_{eff}(\psi, \phi)}{3M_p^2},$$

$$3H\dot{\psi} \approx -\frac{\partial V_{eff}(\psi, \phi)}{\partial \psi}$$

and the same for ϕ . This standard approximation technique is known as the slow-roll approximation, and is the one employed in supernatural inflation.

2.5 Supernatural inflation potential function

At the classical level fields would be found at the potential minimum in equilibrium at zero temperature. However, in the quantum system of scalar fields, this classical statement cannot be true, since the fields would experience quantum fluctuations, and instead the fields evolve to reach their vacuum expectation values, $\langle 0|\Phi|0\rangle$, $\langle 0|\Psi|0\rangle$. Classically, fluctuations in thermal equilibrium would be treated as follows: at non-zero temperature a system of fixed volume will not minimize its potential energy but the Helmholtz free energy, $F = V - TS$. Yet actually calculating the entropy of the quantum system is technically complex, since it involves allowing for quantum interactions with a thermal bath of background particles. As is often the case in problems involving phase transitions, plausibility arguments for the form of the effective potential, $V_{eff}(\Phi, \Psi)$, are given and then checked against experimental bounds. This is the approach taken here.

In general, an inflationary potential should have a quadratic dependence on $|\Phi|$

and $|\Psi|$ near the origin. The simplest models involving supersymmetry breaking give rise to density perturbation predictions far below the observations, and it is therefore essential to have an additional interaction between Φ and Ψ . Under this requirement, one might then assume the existence of a superpotential, W ,

$$W = \frac{\Phi^2 \Psi^2}{2M'} \quad (2.17)$$

which couples the two fields, and is modulated by some characteristic mass scale, M' , equal to M_p , M_{GUT} or some other dynamical scale. In most hybrid inflation models, the Φ field is very light while the Ψ field is very massive. Most supersymmetric models give rise to radiative corrections which generally make Ψ too massive to keep them consistent with observations. However in the supernatural inflation model the masses of the fields, m_Φ and m_Ψ are both on the order of the soft supersymmetry breaking scale, $1TeV$ so this problem does not occur. Assuming that $m_\Phi^2 > 0$ and $m_\Phi^2 < 0$ and the cosmological constant is zero at the minimum of Φ and Ψ an effective supersymmetry breaking potential for the system can be written as,

$$V_{eff}(\Phi, \Psi) = M_I^4 \cos^2\left(\frac{|\Phi|}{M_p}\right) + m_\Psi^2 |\Psi|^2 + \frac{|\Phi|^4 |\Psi|^2 + |\Psi|^4 |\Phi|^2}{M'^2} \quad (2.18)$$

Again, for the purpose of an inflationary model, the scalar fields can be taken to be real. Thus, taking $\Psi \equiv \frac{(\psi + i\psi_1)}{\sqrt{2}}$ and similarly for Φ , the potential for the real fields can be written as,

$$V_{eff}(\phi, \psi) = M_I^4 \cos^2\left(\frac{\phi}{\sqrt{2}M_p}\right) + \frac{m_\psi^2}{2} \psi^2 + \frac{\phi^4 \psi^2 + \psi^4 \phi^2}{8M'^2} \quad (2.19)$$

and is represented graphically in figure 2-2.

Although it may appear as though a very special form for the ϕ potential was used, the cosine function is not required since a Taylor series expansion demonstrates that the constant and mass term are most relevant. The mass scales, M_I and M_p were chosen for consistent inflation and to fit the experimental constraint from density perturbations in the slow-roll regime,

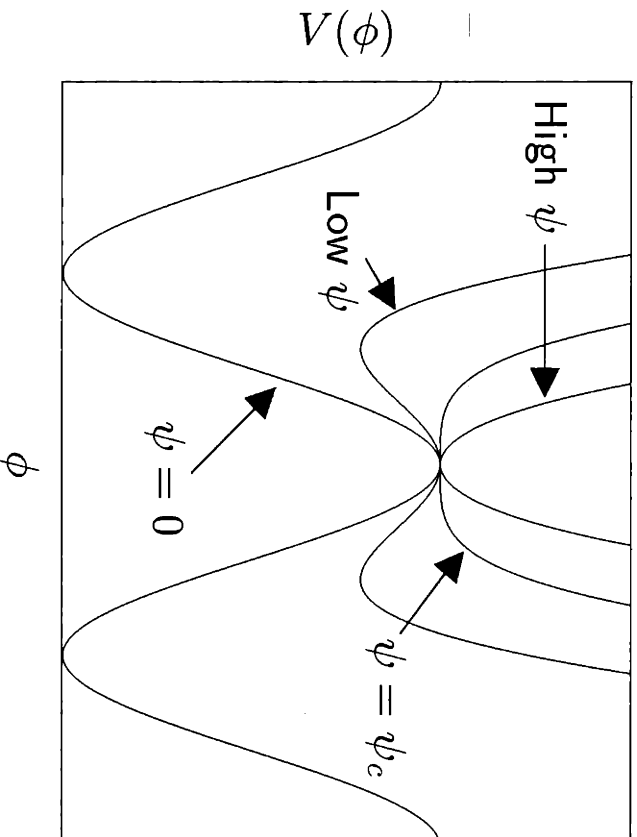


Figure 2-2: Graphical representation of a supernatural inflation potential.

$$\frac{\sqrt{8\pi}V_{eff}^{3/2}}{M_p(dV_{eff}/d\psi)} = 6 \times 10^{-4} \quad (2.20)$$

Although ψ and ϕ might be moduli or standard model flat directions fields, it is assumed that their potentials are very different. The effective potential given is simply an illustrative example of how such a model could work.

2.6 Dynamics of the scalar fields

It is important to give a clear treatment of the dynamics of the scalar fields involved in an inflation model because doing so allows for an accurate determination of the number of e-folds required for inflation to end. When the ψ field is treated classically by considering the expectation value of $\langle\psi\rangle$, the slow-roll approximation is made, and the form of the effective potential in supernatural inflation is used, the equation of motion for the field can be written as,

$$3H\dot{\psi} + m_\psi^2\psi + \frac{\phi^4\psi^2}{4M^2} = 0 \quad (2.21)$$

This equation can be solved to describe the three stages of evolution of the field ψ . The early stage of its evolution is when the ψ field rolls toward the origin, and primordial density perturbations in the field are produced. At this time the ϕ field is so small that the interaction term in equation (2.21) can be neglected. By solving the slow roll equation of motion, ψ is given by,

$$\psi(t) = \psi_c e^{-\frac{\mu_\psi^2 N}{3}} \quad (2.22)$$

where $\mu_\psi = \frac{m_\psi}{H_{inf}}$, $N = Ht$, and $\psi_c = \sqrt{2M^2 m_\phi}$ is the value of ψ when $m_\phi^2 = 0$ (at the origin). As the system evolves, the ϕ field will grow to a sufficiently large critical value, $\phi_c = \sqrt{2M^2 H_{inf}}$. Here the ψ mass becomes large, and the ψ field enters its second stage of evolution where it acts as a coherent state of oscillating particles with $m_\psi(t) = \phi^2/2M^2$. Finally, the ψ field enters its last stage of evolution and begins to decay. To find this, Randall, *et al.* replaced the time evolution of ψ by the time evolution of its envelope, ψ_e at a time sufficiently late that the $\psi^4\phi^2/8M^2$ in the potential can be ignored. The envelope obeys the approximate equation of motion,

$$\dot{\psi}_e = -\left(\frac{3H_{inf}}{2} + \frac{1}{2}\Gamma(t)\right)\psi_e \quad (2.23)$$

where $\Gamma(t)$ is ψ 's decay rate. The time dependence arises from the time dependent mass. The possible identities of ψ are discussed in [17] and using these the super-natural inflation model is constrained under two scenarios for the ψ decay. If ψ has renormalizable couplings to other fields, the decay rate is $\Gamma_b \approx m_\psi(t)$, whereas if the decay rate assumes no renormalizable couplings but Planck suppressed reactions which allow the field to decay the rate could be as small as $\Gamma_l \approx m_\psi(t)^2/(M_p/\sqrt{8\pi})$. The ψ field evolution ends when the amplitude is quickly reduced to zero, only the ϕ

²Note that the argument t is used to distinguish the time-dependent physical mass of ψ particles from the time-independent mass parameter in the potential.

field remains and is marked by the time at which $\Gamma_\psi \approx H_{inf}$.

Because of the strong dependence of the ψ field on $m_\phi(t)^2 = m(\phi)^2(1 - \psi^4/\psi_c^4)$, the ψ evolution is critical in determining the ϕ evolution. Moreover, such a dependence merits the description of the early stage of the ϕ evolution by a Fokker-Planck probability distribution. It is by the considering the exact solution to the Fokker-Planck equation that the correct initial conditions for the subsequent evolution of the classical field equations can be found. These calculations become quite involved and are found in [17], and the results are merely outlined and stated here.

The very early stages of ϕ evolution can be broken into the quasi-equilibrium and diffusive regimes. The transition from the diffusive to the classical regime is relevant to inflation and occurs at a time, $N_0 \simeq w\sqrt{9/8}$, where $w = 1/\mu_\psi\mu_\phi = H_{inf}^2/m_{\phi_q}m_\phi$. After this time the classical evolution of ϕ can be determined very well analytically and again the analysis can be divided into three stages, according to the behavior of ψ . The equation of motion for ϕ at early times is solved by,

$$\phi(N) = \bar{\phi}_i e^{2(N-N_0)^2/9w^2} \quad (2.24)$$

where $\bar{\phi}_i = \frac{H_{inf}}{2\pi}(9\pi ew^2)^{1/4}$. This stage lasts for a time $N_1 \approx w\sqrt{9/8}\sqrt{\log(\phi_c/\bar{\phi}_i)}$ e-folds, where $\phi_c = \sqrt{2M'H_{inf}}$, and M' is some large mass scale approximately equal to the Planck, GUT or intermediate scale. Next, during the ψ -oscillatory stage the $\psi^4\phi^2$ term is negligible and ϕ keeps up with the minimum of the potential such that

$$\phi(N) = \sqrt{m_\phi M'} e^{3N/2} \quad (2.25)$$

and lasts until the ψ fields decays. For a ψ with decay constant Γ_b this lasts for a time $N_2^b \simeq 0$. If the ψ decay constant is Γ_l , the value of the ϕ field when ψ decays is $\phi_l = (H_{inf}M'^3M_p^2/\pi)^{1/6}$. The total number of e-folds in this case is approximately $N_2^l = 2/3(\phi_l/\phi_c) = (1/9)\log(M_p^2/8H^2\pi)$. After ψ decays, ϕ follows the $\psi = 0$ equation of motion according to

$$\phi(t) \propto e^{rN} \quad (2.26)$$

where

$$r = \sqrt{\mu_\phi^2 + \frac{9}{4}} - \frac{3}{2} \quad (2.27)$$

The number of e-folds in this stage is $N_3 \simeq (1/r) \log(\pi M_p / \sqrt{2} / \{\phi_e, \phi_l\})$, depending on the decay rate.

Knowing the number of e-folds is required because it must be that the density fluctuations relevant for the observed physical scales have exited the horizon while the ϕ field is in its early quasi-equilibrium stage. The quantum fluctuations in the ϕ field during its diffusive regime generate a spike in the density perturbation.

The initial density perturbations are generated both in the ψ and the ϕ fields due to quantum effects. One interpretation of the source of these density perturbations is that inflation ends at different times at different points in space. The quotient of the time delay function, $\Delta\tau(x)$, with the characteristic cosmological time scale, H_{inf}^{-1} , is of the order of the density perturbation, $\frac{\delta\rho}{\rho}$, at the time the wavelength re-enters the Hubble length.

In the case of the ψ field, this is given by

$$\left(\frac{\delta\rho}{\rho}\right)_\psi \approx H_{inf} \Delta\tau = H_{inf} \frac{\Delta\psi}{\psi} \quad (2.28)$$

With $\Delta\psi \approx \frac{H_{inf} l}{2\pi}$,

$$\left(\frac{\delta\rho}{\rho}\right)_\psi \approx \frac{H_{inf}^2}{2\pi |\psi|} \quad (2.29)$$

Taking the derivative of equation (2.22) yields,

$$|\dot{\psi}| = \frac{3H_{inf}}{2\pi\mu_\psi^2} \frac{1}{\sqrt{2M' m_\phi}} e^{-\frac{\mu_\psi^2 H_{inf} t}{3}} \quad (2.30)$$

Primordial density perturbations generated by the ψ field are therefore given by,

$$\left(\frac{\delta\rho}{\rho}\right)_\psi \approx H_{inf} \Delta\tau = \frac{H_{inf} \mu_\psi^2 \sqrt{2M' m_\phi}}{3} e^{\frac{\mu_\psi^2 H_{inf} t}{3}} \quad (2.31)$$

Note that $\psi \sim e^{-m_\psi^2 N/3H_{inf}}$ and $\Delta\psi \sim H_{inf}/2\pi$ fit the density fluctuation constraint

given in equation (2.20).

The density perturbations generated by the ϕ field are given by,

$$\left(\frac{\delta\rho}{\rho}\right)_\phi \approx H_{inf}\Delta\tau = H_{inf}\frac{\Delta\psi}{\psi} \quad (2.32)$$

Because the ϕ evolution is complicated by the ψ evolution, the reader should refer to [17] for details. Primordial density perturbations generated by the ϕ field are

$$\left(\frac{\delta\rho}{\rho}\right)_\phi \approx H_{inf}\Delta\tau = \left(\frac{9}{\pi}\right)^{1/4}\frac{3}{2N_e}w^{3/2}e^{-2N_{fi}^2/9w^2} \quad (2.33)$$

where N_{fi} is the time at which the fluctuation occurs and N_e is the time at which inflation ends and the classical evolution takes over. It is given by,

$$N_e = N_0 + N_1 + N_2 + N_3 \quad (2.34)$$

Note that the density perturbations in ϕ is given by a Gaussian which falls off from its peak at $N_{fi} = 0$ with width $\sqrt{9w^2/2}$.

For supernatural models to be viable it is important that this spike is generated at short wavelengths (scales of $1Mpc$ or less) so as to avoid conflict with large scale structure observations. Density fluctuations on the scale of $1Mpc$ are formed at,

$$\Delta N_{1Mpc} = 38 + \frac{2}{3}\log(M/10^{11}) + \frac{1}{3}\log(T_{RH}/10^7) \quad (2.35)$$

where M is a particle physics scale under investigation and T_{RH} is the reheat temperature of the universe at this scale [10].

In this two field inflation model, the energy and entropy source is the decay of the ψ and ϕ fields. As discussed above, the ψ field decays first, and the decay products are assumed to be quickly thermalized, giving an effective temperature, T_ψ . Later, the ϕ field reaches the minimum of its potential and oscillates about it. These oscillations are damped by either gauge or Yukawa couplings. The decay leads to a

reheat temperature given by,

$$T_{RH} = \max(g^{2/3} m_\phi^{5/6} M^{1/6}, m_\phi/\sqrt{\lambda}) \quad (2.36)$$

where λ is the Yukawa coupling constant and g is a gauge coupling constant [18]. In this study, the gauge coupling constant is taken as unity and the gauge coupling is therefore dominant, making

$$T_{RH} = g^{2/3} m_\phi^{5/6} M^{1/6}. \quad (2.37)$$

In figures (2-3), (2-4) and (2-5) the values of the supernatural inflation model class parameters, m_ψ , m_ϕ , μ_ψ^{-1} , μ_ϕ , and H during inflation, are plotted when the larger inflaton field decay rate, $\Gamma(t) = \Gamma_b$, is used, and M' is approximately M_p , M_{GUT} and M_I , respectively. The values shown were found by imposing the criterion for the correct magnitude of density fluctuations (equation (2.20)) and choosing the minimum $\mu_\phi \equiv m_\phi/H_{inf}$ consistent with a sufficiently rapid end to inflation, *i.e.* $N_e < N_{1Mpc}$ by $5w$. The range of M plotted in these figures was chosen noting that smaller M would increase the values of $1/\mu_\psi$ and μ_ϕ and large M would decrease these values but would make the masses uncomfortably large relative to the TeV scale.

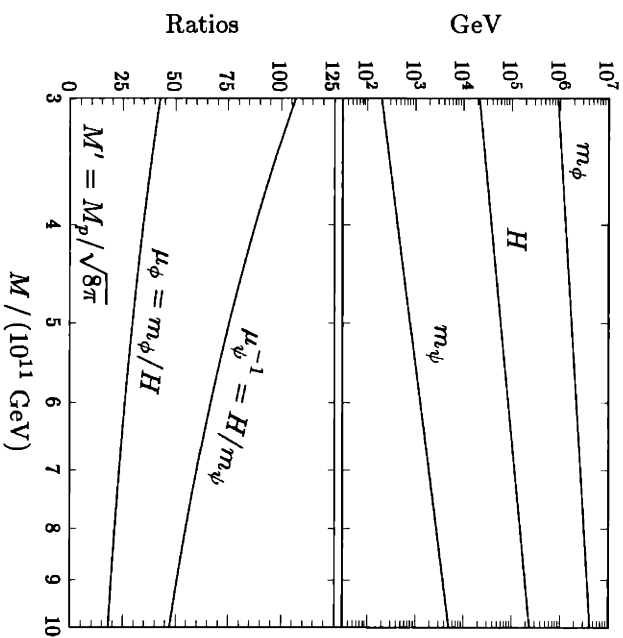


Figure 2-3: Parameter choices for supernatural inflation with M' at the Planck scale. Here μ_ψ is chosen to give the correct magnitude of density fluctuations for the minimum μ_ϕ consistent with a sufficiently rapid end to inflation.

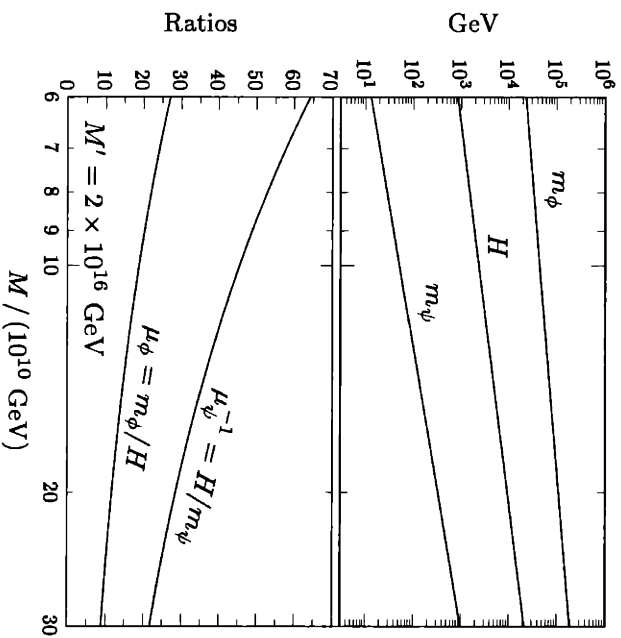


Figure 2-4: Parameters for supernatural inflation with M' at the GUT scale. The values were chosen by the same criteria used in figure (2-3).

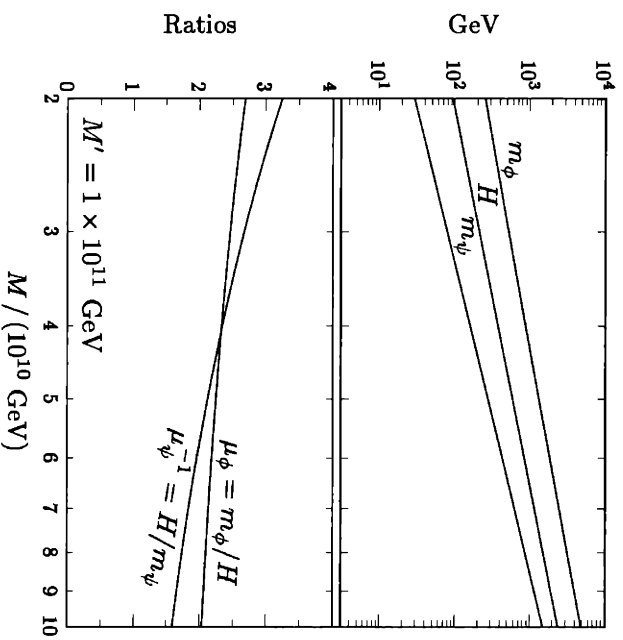


Figure 2-5: Parameters for supernatural inflation with M' at the intermediate scale. The values were chosen by the same criteria used in figure (2-3).

Chapter 3

CMB Anisotropy Formation

“The vastness of the heavens stretches my imagination – stuck on this carousel my little eye can catch one-million-year-old light. A vast pattern – of which I was a part – perhaps my stuff was belched from some forgotten star, as one is belching there . . . It does not do harm to the mystery to know a little about it. Far more marvelous is the truth than any artists of the past imagined!”

- *The Feynman Lectures on Physics*– Richard P. Feynman

3.1 Overview

The key idea in studying structure formation in the universe is that of gravitational instability. Stated simply, if the material in the universe is distributed irregularly, then the overdense regions provide extra gravitational attraction and draw material toward them, and thus become more overdense. In the current epoch, astronomers have found that on moderate scales (less than 10 Mpc), the material in the universe is very unevenly distributed and is found in the form of galaxies and quasars. At very early times, by contrast, CMB observations indicate that the universe was distributed much more evenly. Indeed, at the last scattering redshift, ($z \approx 1000$), gravitational instability theory dictates that fractional density perturbations $\frac{\delta\rho}{\rho} = \delta \geq 10^{-3}$ must

have existed in order for galaxies and clusters to have formed by the present. The details of the gravitational instability process depend on the nature of the universe as a whole¹, and the form of the initial irregularities. Inflation is the only theory which provides an explanation for the origin of these initial irregularities that is consistent with the current data[8].

Primary anisotropies are those that arise due to effects at recombination. Secondary anisotropies are generated by scattering along the line of sight. There are three basic primary effects which are important on, respectively, large intermediate and small angular scales:

1. Gravitational (Sachs-Wolfe) perturbations. Photons from high-density regions at last scattering have to climb out of potential wells, and are thus redshifted.
2. Intrinsic (adiabatic) perturbations. In high-density regions, the coupling of matter and radiation can compress the radiation also, giving a higher temperature.
3. Velocity (Doppler) perturbations. The plasma has a non-zero velocity at recombination, which leads to Doppler shifts in frequency and hence brightness temperature.

Under the “big bang” model for cosmology, before redshift $z = 1000$, photons in the Cosmic Microwave Background (CMB) were hotter by a factor of $(1+z)$ and hence were able to ionize the hydrogen in the universe. Compton scattering of photons and electrons tightly couples the two species. In addition electromagnetic interactions couple the electrons and baryons together. This photon-electron-baryon system thus can be thought of as a single tightly coupled fluid, which is called the photon-baryon fluid for short to identify the dominant dynamical components. After the “recombination” epoch at $z = 1000$ when neutral hydrogen formed, CMB photons mainly just streamed toward the observer at the present. Hence temperature differences on this surface of last scattering become the anisotropies in the CMB temperature seen today.

¹ *e.g.* the matter content and Hubble parameter of the universe

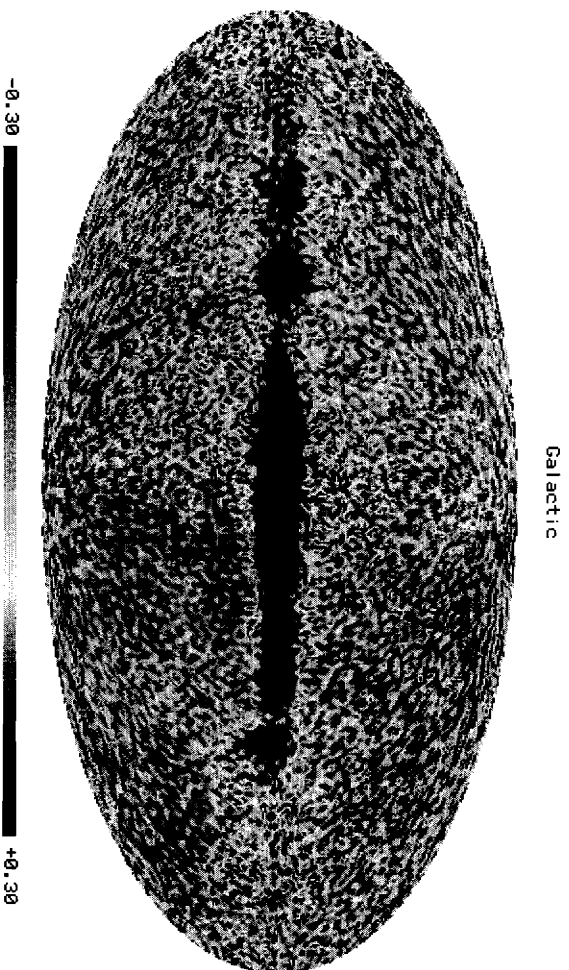


Figure 3-1: This figure is a preliminary map of a collaborative effort (involving A.J. Banday, K.M. Górski, G. Hinshaw and A. Kogut) to make COBE-DMR four year sky maps in the Healpix format [6] (see also <http://www.tac.dk/~healpix/skymaps1.html>). This map is shown in Galactic coordinates, and was made at a higher resolution than the previously released public maps smoothed to an effective beam resolution of 10 degrees. It is shown in mK .

It is believed that large scale structure in the universe grew out of small perturbations in the early universe through gravitational instability. This implies that the photon-baryon fluid moves in a gravitational potential well before last scattering.

- 2 The response of the fluid to the gravitational potential fluctuations allow one to measure the properties of the fluid in an expanding universe known to be filled with dark matter. This also allows one to extract basic cosmological parameters, as well as those of the seed perturbations, which can be used to pin down the nature of large scale structure formation in the universe.

To extract this sort of information a map of the CMB sky such figure (3-1) must be analyzed. This basically involves taking the power spectrum of this primordial noise. Since the fluctuations are on the sky, this amounts to taking an angular decomposition of the fluctuations in multipole space ℓ (proportional to the inverse angle) rather

²This assumes a Newtonian representation of perturbations or gauge.

than Fourier space k (where the underlying potential fluctuations exist). When this is done with the data available at the present time, the angular power spectrum of CMB anisotropies results.

3.2 Cosmological perturbations

Quantum fluctuations of the supernatural inflation fields, ψ and ϕ are given by,

$$\delta\psi(\mathbf{x}, t) = \sum_{\mathbf{k}} \delta\psi_{\mathbf{k}}(t) e^{i\mathbf{k}\cdot\mathbf{x}} \quad (3.1)$$

$$\delta\phi(\mathbf{x}, t) = \sum_{\mathbf{k}} \delta\phi_{\mathbf{k}}(t) e^{i\mathbf{k}\cdot\mathbf{x}} \quad (3.2)$$

where $\delta\psi_{\mathbf{k}}$ and $\delta\phi_{\mathbf{k}}$ are the Fourier components corresponding to each vacuum fluctuation. The variable \mathbf{x} is related to the physical position \mathbf{r} by $\mathbf{r} = a(t)\mathbf{x}$, giving the physical wavenumber as k/a . The inverse of the physical wavenumber, a/k defines a distance scale correlated with the expansion, which is specified by its current value, $1/k$. A scale is inside the horizon if $aH/k < 1$ and outside if greater than unity. Scales of interest leave the horizon during inflation and re-enter it after inflation ends.

The perturbations, $\delta\psi(\mathbf{x}, t)$ and $\delta\phi(\mathbf{x}, t)$ lead to a perturbation in the energy density, $\delta\rho(\mathbf{x}, t)$, and hence the space-time metric. After inflation when the fields decay into matter, there will be inherent perturbations in the densities of each particle species, $\delta\rho_i(\mathbf{x}, t)$. Finally there will also be a more complicated perturbation $\Theta(t, \mathbf{x}, \mathbf{n})$ in the function specifying the number of photons at position \mathbf{x} , with momentum direction \mathbf{n} , known as the CMB anisotropy.

All perturbations are specified by $\delta\psi(\mathbf{x}, t)$ and/or $\delta\phi(\mathbf{x}, t)$, and when Fourier expanded can be written as,

$$T_g(t, k) \{ \delta\phi_{\mathbf{k}}(t_*) + \delta\psi_{\mathbf{k}}(t_*) \} \quad (3.3)$$

where T_g is the transfer function for a generic perturbation and is fixed by the current

value of the Hubble parameter, H_0 , and the baryon density, Ω_b .³

However, $\delta\psi(\mathbf{x}, t)$ and $\delta\phi(\mathbf{x}, t)$ are not necessarily the most useful quantities for describing the evolution of perturbations because they are not constant outside the horizon, and after the scalar fields decay these quantities cease to exist. A more useful quantity is the curvature perturbation $\mathcal{R}_\mathbf{k}$, which is constant outside the horizon, and still remains well defined even after ψ and ϕ decay. It can be shown that \mathcal{R} is the scalar spatial perturbation of the Friedmann-Robertson-Walker metric in any slicing that is comoving and is related to the vacuum fluctuations and Hubble parameter by,

$$\mathcal{R}_\mathbf{k} = - \left(\frac{H_{inf}}{q} \right) \delta\psi_\mathbf{k} = H\delta t \quad (3.4)$$

and similarly for ϕ .

3.3 Multipoles

Photons are characterized by the number of photons per quantum state, or occupation number. Ignoring perturbations, the occupation number is a function of the magnitude of the photon momentum and in the case of the CMB is given by a blackbody distribution,

$$f(p) = \frac{1}{e^{p/T} - 1}, \quad (3.5)$$

where $T = 2.728K$. Perturbations to $f(p)$ are magnitude and direction dependent, and the total is given by,

$$f(\mathbf{p}) = f(p) + \delta f(\mathbf{p}). \quad (3.6)$$

It can be shown (c.f. [12]) that to first order in perturbations $f(\mathbf{p})$ is a blackbody distribution, with a fractional temperature perturbation, $\delta T/T$ that is independent of the magnitude of the photon momentum, p but does depend on the direction \mathbf{n} of the photon momentum, or equivalently, the direction of observation, $\mathbf{e} = -\mathbf{n}$. Thus

³Note that T_g is independent of \mathbf{k} because the evolution equations are invariant under rotations, and that depending on the context, various prefactors are factored out before defining the transfer function. However, it is often defined to approach unity on large scales.

the fractional temperature perturbation, $\delta T/T(\mathbf{e})$ is given by,

$$\frac{\delta T(\mathbf{e})}{T} = \sum_{\ell, m} a_{\ell m} Y_{\ell m}(\mathbf{e}) \quad (3.7)$$

where $a_{\ell m}$ are the multipoles of the cosmic microwave background anisotropy, and $Y_{\ell m}(\mathbf{e})$ are the spherical harmonics. Although the monopole a_{00} is well-defined if a position-dependent δT is considered, there is no way of measuring it. The dipole would also vanish if observers measured it from the rest frame⁴ of the CMB. However it does not vanish because of the Doppler shift, $\mathbf{e} \cdot \mathbf{v}$ where \mathbf{v} is the Earth's velocity relative to the CMB rest frame. Note that the multipoles with $\ell \geq 2$ represent the intrinsic anisotropy of the cosmic microwave background.

Because the equations are linear and invariant under rotations, CMB multipoles must be of the form (see [12]),

$$a_{\ell m} = \frac{4\pi}{(2\pi)^{3/2}} \int_0^\infty T_{\Theta}(k, \ell) \mathcal{R}_{\ell m}(k) k dk \quad (3.8)$$

Note the CMB transfer function, $T_{\Theta}(k, \ell)$ must be independent of m because of this invariance.

The ensemble mean variance of the CMB multipoles defines the quantity, C_ℓ , the spectrum of the cosmic microwave background. It can be written as,

$$C_\ell = \sum_m \langle |a_{\ell m}|^2 \rangle = 4\pi \int_0^\infty T_{\Theta}^2(k, \ell) \{ \mathcal{P}_{\mathcal{R}_\psi}(k) + \mathcal{P}_{\mathcal{R}_\phi}(k) \} \frac{dk}{k} \quad (3.9)$$

When the slow-roll approximation is used the primordial curvature spectra, $\mathcal{P}_{\mathcal{R}_\psi}(k)$ and $\mathcal{P}_{\mathcal{R}_\phi}(k)$ are given by,

$$\mathcal{P}_{\mathcal{R}_\psi}(k) = \left(\frac{H_{inf}}{q_\psi} \right)^2 \mathcal{P}_\psi \Big|_{t=t_*} \quad (3.10)$$

$$\mathcal{P}_{\mathcal{R}_\phi}(k) = \left(\frac{H_{inf}}{\phi} \right)^2 \mathcal{P}_\phi \Big|_{t=t_*} \quad (3.11)$$

⁴This is defined as the frame in which the momentum density vanishes.

where t_* is a few Hubble times after the epoch of horizon exit, given by $k = aH$. Assuming that $\delta\phi_{\mathbf{k}}$ and $\delta\psi_{\mathbf{k}}$ are practically free fields, slow-roll applies such that they both turn out to have negligible mass, and both will generate a Gaussian vacuum fluctuation. A few Hubble times after horizon exit, these fluctuations tend to the values,

$$\mathcal{P}_\psi = \mathcal{P}_\phi = \left. \left(\frac{H_{inf}}{2\pi} \right)^2 \right|_{k=aH} \quad (3.12)$$

Combining equations gives the spectrum of primordial curvature perturbations,

$$\mathcal{P}_{\mathcal{R}_\psi}(k) = \left[\left(\frac{H_{inf}}{\psi} \right) \left(\frac{H_{inf}}{2\pi} \right) \right]_{k=aH}^2 \quad (3.13)$$

$$\mathcal{P}_{\mathcal{R}_\phi}(k) = \left[\left(\frac{H_{inf}}{\phi} \right) \left(\frac{H_{inf}}{2\pi} \right) \right]_{k=aH}^2 \quad (3.14)$$

Comparing these equations with those of chapter 2 yields,

$$\mathcal{P}_{\mathcal{R}_\psi}(k) = \left(\frac{\delta\rho_\psi}{\rho_\psi}(k) \right)^2 = \left[\frac{3H_{inf}}{2\pi\mu_\psi^2} \frac{1}{\sqrt{2M' m_\phi}} \left(\frac{k}{k_{peak}} \right)^{\mu_\psi^2/3} \right]^2 \quad (3.15)$$

$$\mathcal{P}_{\mathcal{R}_\phi}(k) = \left(\frac{\delta\rho_\phi}{\rho_\phi}(k) \right)^2 = \left[\frac{27w^3}{16\sqrt{\pi}N_e^2} e^{-(\log(k/k_{peak})/3w)^2} \right]^2 \quad (3.16)$$

where $k_{peak} = e^{(\Delta N_{1, Mpc} - N_e)}$. Thus the CMB spectrum under the supernatural inflation model is given by the function,

$$C_l = 4\pi \int_0^\infty T_\Theta^2(k, \ell) \left[\left(\frac{\delta\rho_\psi}{\rho_\psi}(k) \right)^2 + \left(\frac{\delta\rho_\phi}{\rho_\phi}(k) \right)^2 \right] \frac{dk}{k} \quad (3.17)$$

Chapter 4

CMB Temperature spectrum computation

“This summer I have discovered something that is totally useless.”

- Peter Higgs, in a 1964 note to his research student.

4.1 CMBFAST and modifications

Calculating the cmb transfer functions requires calculation of multipoles $\ell \geq 2$ to represent the intrinsic anisotropy of the microwave background. To do this the Boltzmann hierarchy must be solved to sufficiently high order. While codes have been written to solve these equations ([4],[9],[13]), they are much too slow to permit an exploration of the parameter space. Even in codes where reionization is assumed to be negligible (which is unlikely anyway) solving the Boltzmann hierarchy is still much too slow.

A more efficient approach is to express the temperature transfer function as an integral along the photon past light cone. This is known as the line of sight method and is the one employed in CMBFAST [19]. The temperature transfer function using

this method is given by,

$$T_{\Theta}(k, \ell) = \int_0^{\tau_0} S_{\Theta}(k, \tau) \eta_{\ell} [k(\tau_0 - \tau)] d\tau. \quad (4.1)$$

The main advantage of the line of sight integration method is that the anisotropy is decomposed into a source term, $S_{\Theta}(k, \tau)$ which is independent of the multipole moment ℓ and a geometrical term η_{ℓ} , which is independent of the particular cosmological model. The geometrical term can thus be computed only once and stored for subsequent calculations. The source term is the same for all multipole moments and only depends on small number of contributions from the gravitational potential, baryon velocity and photon moments up to $\ell = 2$.

When CMBFAST was first introduced, few two-field inflation models had been developed. Thus, CMBFAST was designed for single inflation models and sets the default primordial power spectrum to a pure power law, k^n . To accommodate two-field models supernatural inflation models, the primordial power spectrum was replaced with,

$$\mathcal{P}_{\mathcal{R}_{modified}}(k) = \mathcal{P}_{\mathcal{R}_{\psi}}(k) + \mathcal{P}_{\mathcal{R}_{\phi}}(k) \quad (4.2)$$

where $\mathcal{P}_{\mathcal{R}_{\psi}}(k)$ represents the power law portion of the spectrum and $\mathcal{P}_{\mathcal{R}_{\phi}}(k)$ is the spike generated.

4.2 Checking the magnitude of fluctuations

To check the magnitude of fluctuations for different values of the w parameter, ($w = 1/\mu_{\psi}\mu_{\phi} = H_{inf}^2/m_{\psi}m_{\phi}$), the ratio of the value of $\delta\rho_{\phi}/\rho_{\phi}$ ($N = N_e - 40$) to $6 \times 10^{-4}/2\pi\sqrt{3}$, the maximum value of $\delta\rho_{\phi}/\rho_{\phi}$ that is consistent observation was calculated¹. Using this quantity (called Δ) estimates for the magnitude of $\mathcal{P}_{\mathcal{R}_{\phi}}(k)$ at the scale of $1Mpc$ can be made. The results of these calculations are summarized in figure (4-1). In principle values of w which give $\Delta > 1$ are excluded by observation.

¹The quantity 40 is taken as an estimate of N_{1Mpc} . If N_{1Mpc} is calculated using equation (2.35) this leads to an error of approximately 1.5.

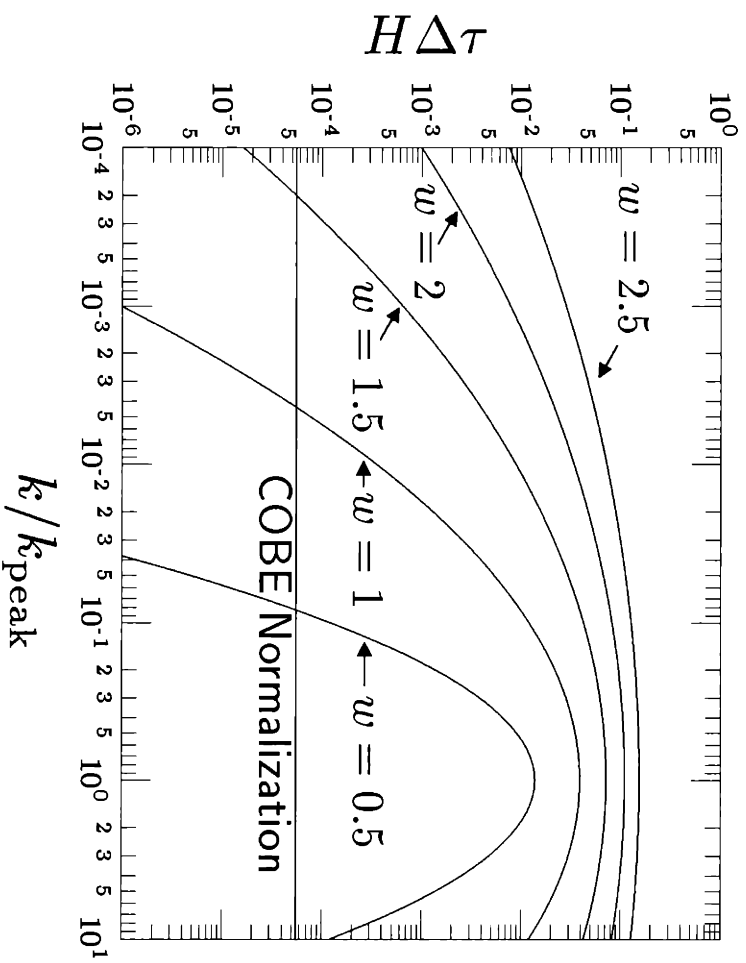


Figure 4-1: The magnitude of the spike generated by the ϕ field in supernatural inflation. The horizontal line represents the Peebles-Harrison-Zeldovich spectrum characteristic of COBE data.

Table 4.1: Energy Scales of Peak Parameters in Supernatural Inflation

Parameters	Planck Scale	GUT Scale	Intermediate scale
w	$2.5 \leq w \leq 2.6$	$2.4 \leq w \leq 2.5$	$0.78 \leq w \leq 1.2$
N_e	$24.8 \leq N_e \leq 25.5$	$23.4 \leq N_e \leq 24.7$	$25.4 \leq N_e \leq 27.3$
Δ	$.89 \leq \Delta \leq 3.02$	$0.06 \leq \Delta \leq 0.46$	$6.12 \times 10^{-10} \leq \Delta \leq 1.87 \times 10^{-8}$

However, because Δ changes very quickly as the parameters are varied, only a very small change in parameters would be needed to make $\Delta = 1$. Table (4.1) shows the energy scales that the w parameter correspond to in figure (4-1).

4.3 Calculating the CMB spectrum

CMBFAST requires the input of several cosmological parameters, $H_0, \Omega_b, \Omega_c, \Omega_\Lambda, \Omega_p, \tau, Y_{He}, T_0$ and the inflationary parameter, n_s . Recent analysis by Lange *et. al* ([11]), has determined first estimations of the first six of these parameters. Among their conclusions is that the Boomerang 98 (B98) data[5] (see figure 4-2) are consistent with the prediction of the basic inflationary paradigm: the curvature of the universe is near zero ($\Omega_k = 0$) and that the primordial power spectrum is nearly scale invariant ($n_s = 1$). In addition, the slight preference that the data shows for closed rather than open models is not, in their opinion, statistically significant. Their study explicitly illustrated how inferences that are drawn from CMB and other data depend on the prior probability weights of the parameters. Table (4.2) lists some of their findings.

Supernatural inflation models assume a flat geometry for the universe, *i.e.* $\Omega_{flat} = 1$. Using this as a strongly restrictive criterion, the values of the first six cosmological parameters in the above list can be taken from entries $P10, P11$ and $P13$ of table (4-2).

The values of the remaining CMBFAST input parameters were taken from [23] as $T_0 = 2.728K$ and $Y_{He} = 0.24$. The scalar spectral index, n_s , was calculated using the relation,

$$n_s = 1 - 2\alpha_s \quad (4.3)$$

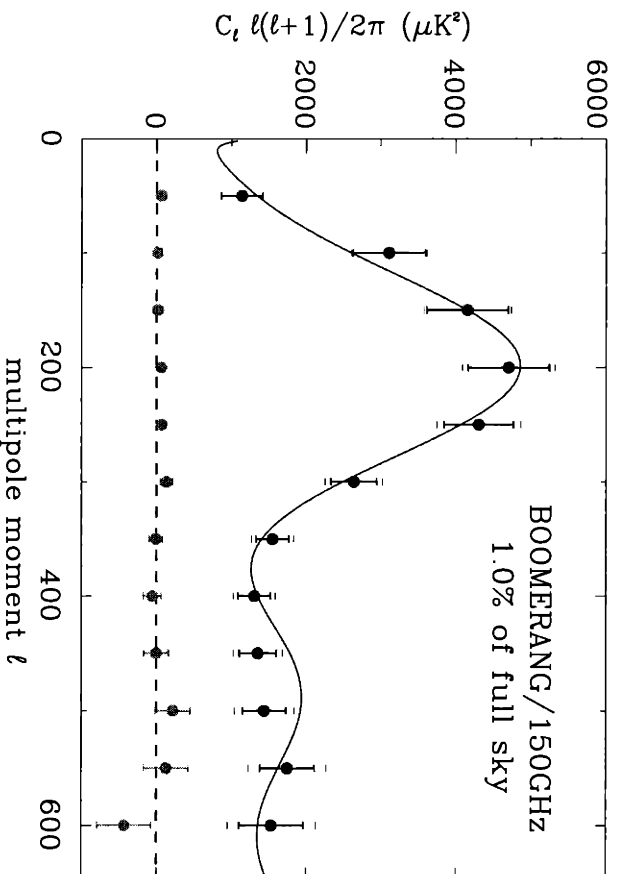


Figure 4-2: Angular power spectrum measured by Boomerang at 150 GHz, taken from [5]. Each point is the power averaged over $\Delta\ell = 50$ and has negligible correlations with the adjacent points. The error bars indicate the uncertainty due to noise and cosmic/sampling variance. The errors are dominated by cosmic/sampling variance at $\ell < 350$; they grow at large ℓ due to the signal attenuation caused by the combined effects[3] of the 10' beam and the 14' pixelation (0.87 at $\ell = 200$ and 0.33 at $\ell = 600$). The current $\pm 10\%$ uncertainty in the calibration corresponds to an overall re-scaling of the y -axis by $\pm 20\%$, and is not shown. The current 1' uncertainty in the angular resolution of the measurement creates an additional uncertainty—indicated by the distance between the ends of the red error bars and the blue horizontal lines—that is completely correlated and is largest (11%) at $\ell = 600$. The green points show the power spectrum of a difference map obtained as follows: the data was divided into two parts, corresponding to the first and second halves of the time stream. Two maps (*A* and *B*) were made from these halves, and the green points show the power spectrum computed from the difference map, (*A* – *B*/2). Signals originating from the sky should appear in this map, so this is a test for data contamination. The solid curve has parameters ($\Omega_b = 0.05$, $\Omega_m = 0.31$, $\Omega_\Lambda = 0.75$, $n_s = 0.95$, $h = 0.70$), and is the best model fit for the Boomerang test flight data [14, 15], and is shown for comparison only.

Table 4.2: This table is a sample of some results of parameter extraction using the method of successfully more restrictive priors. The confidence intervals are 1σ . The 2σ values are approximately double the 1σ values quoted in most cases; upper limits are quoted at 2σ . The quoted values are reported after marginalizing over all other parameters. The weak h priors are tophat functions (uniform priors) and include an additional age $> 10Gyr$ prior. The LSS priors are combinations of Gaussians and tophats. Columns 1-5 (Ω_{tot} to Ω_Λ) are predominantly driven by the CMB data, except for $\Omega_b h^2$ and Ω_b when the strong BBN prior is applied. Most of the parameters in columns 6-10 (τ_c to Age) are influenced by the structure of the parameter space and should not be interpreted as CMB-driven constraints; exceptions are the $\Omega_c h^2$ and Ω_Λ results when the LSS prior is applied.

Priors	Ω_{tot}	$\Omega_b h^2$	n_s	Ω_b	Ω_Λ	τ_c	$\Omega_c h^2$	Ω_m	h	Age
P10: $\Omega_{tot} = 1$ & Weak $h+$ age	1	$0.031_{0.004}^{0.004}$	$0.990_{0.07}^{0.07}$	$0.060_{0.02}^{0.02}$	< 0.78	$0.100_{0.07}^{0.13}$	$0.270_{0.07}^{0.05}$	$0.570_{0.21}^{0.21}$	$0.740_{0.09}^{0.09}$	$10.90_{0.8}^{0.8}$
P11: $\Omega_{tot} = 1$ & LSS & Weak	1	$0.030_{0.004}^{0.004}$	$0.960_{0.06}^{0.07}$	$0.050_{0.01}^{0.01}$	$0.670_{0.06}^{0.04}$	$0.090_{0.07}^{0.12}$	$0.180_{0.02}^{0.02}$	$0.370_{0.07}^{0.07}$	$0.790_{0.05}^{0.05}$	$11.70_{0.4}^{0.4}$
P13: $\Omega_{tot} = 1$ & LSS & Weak & SNIa	1	$0.030_{0.003}^{0.003}$	$0.970_{0.06}^{0.07}$	$0.050_{0.01}^{0.01}$	$0.690_{0.02}^{0.04}$	$0.100_{0.07}^{0.12}$	$0.180_{0.01}^{0.02}$	$0.310_{0.03}^{0.03}$	$0.810_{0.03}^{0.03}$	$11.60_{0.3}^{0.3}$

where, according to [17], $\alpha_s = -\mu_\psi^2/3$. For these models n_s is always greater than 1 and is very close to 1 at both the Planck and GUT scales. This differs from the usual prediction for new or chaotic inflation models.

For M' at the Planck or GUT scales, n_s does not deviate from unity when calculated using the the range of μ_ψ in figures (2-3) and (2-3). However, when n_s is calculated from figure (2-5), it deviates much more from unity and is given by, $1.06 \leq n_s \leq 1.27$. Using Lange *et al*'s approximation that the 2σ error is approximately double the 1σ values quoted in table (4-2), and taking $\Omega_{tot} = 1$ as a strong criteria, the supernatural inflation model at the intermediate scale with the inflaton field decay rate at Γ_b is untenable for $M > 4.3 \times 10^{10} GeV$. This cuts the allowed parameter space of figure (2-5) to less than half by the above restrictions and the corresponding range of the scalar spectral index to $1.06 \leq n_s \leq 1.13$.

The CMB temperature anisotropy spectrum was calculated for values of the supernatural inflation parameters μ_ψ and μ_ϕ in each of figures (2-3), (2-4) and (2-5) where Δ was maximum. These were compared against calculations done without including $\mathcal{P}_{\mathcal{R}_\phi}(k)$ and those calculated using the default CMBFAST power-law primordial spectrum with the input n_s calculated using equation (4.3). The results can

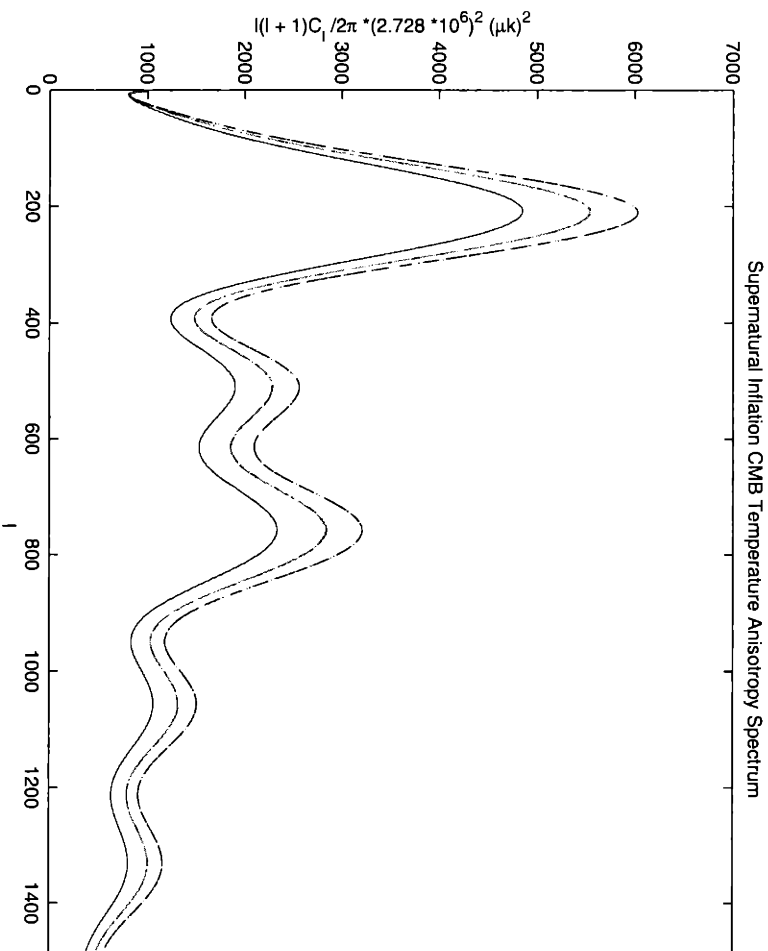


Figure 4-3: In all the curves which appear above, the following cosmological parameters were used: ($\Omega_{tot} = 1$, $\Omega_b = 0.04$, $\Omega_c = 0.26$, $\Omega_\Lambda = 0.04$, $\tau_e = 0.025$, $T_0 = 2.728K$, $Y_{He} = 0.24$). The top curve is the CMB temperature anisotropy spectrum for supernatural inflation at the intermediate scale using either the CMBFAST default $\mathcal{P}_{\mathcal{R}}(k)$ with $n_s = 1.0332$, $\mathcal{P}_{\mathcal{R}\psi}(k)$, or $\mathcal{P}_{\mathcal{R}modified}(k)$. The middle curve was calculated in the same way for supernatural inflation at the GUT or Planck scales, with $n_s = 1.00$. The bottom curve is a reproduction of the the Lange, *et. al* P11 curve, [11].

be found in figure (4-3).

Figure (4-3) illustrates that when the inflaton field decays at a very large rate, Γ_b , the effect of the spike in the primordial perturbation spectrum on the CMB temperature anisotropy spectrum is negligible.

4.4 Discussion

Although the peak generated by the ϕ field in supernatural inflation has a very large amplitude, it is generated at such small scales that it is negligible for CMB obser-

vations. In addition, although this peak is very wide in ℓ space, its effects on the CMB temperature anisotropy are unobservable at the scale of $1Mpc$. However, it is important to note that the above statements only hold for supernatural inflation with a nonrenormalizable superpotential, assuming the larger decay rate. Randall, *et al* suggest that N_e for the same parameters is generally about 5 larger using the smaller decay rate Γ_e , when accompanied by a modest change in μ_ϕ . Although supernatural inflation at the intermediate scale is favored by Randall, *et al* in the context of supersymmetric models, it is the most tightly constrained by current data, and future CMB experiments will establish a value for n_s to the ± 0.01 level, which will constrain the parameter space of supernatural inflation at the intermediate scale even more tightly.

“Somehow, after I finish [writing] a book I always dislike it and can only think of how it should have been better done.”

- Noam Chomsky, personal correspondence.

References

- [1] Andreas Albrecht et al. New inflation in supersymmetric theories. *Nucl. Phys.*, B229:528, 1983.
- [2] D. Bailin and A. Love. *Supersymmetric Gauge Field Theory and String Theory*. Institute of Physics Publishing, Bristol, UK, 1994.
- [3] C. L. Bennett et al. Cosmic temperature fluctuations from two years of COBE DMR observations. *Astrophys. J.*, 436:423–442, 1994.
- [4] J.R. Bond and G. Efstathiou. *Mon. Not. R. Astron. Soc.*, 226:665, 1987.
- [5] P. de Bernardis et al. A flat universe from high-resolution maps of the cosmic microwave background radiation. *Nature*, 404:955–959, 2000.
- [6] Krzysztof M. Gorski, Benjamin D. Wandelt, Frode K. Hansen, Eric Hivon, and Anthony J. Banday. The HEALPIX primer. 1999.
- [7] Alan H. Guth. The inflationary universe: A possible solution to the horizon and flatness problems. *Phys. Rev.*, D23:347–356, 1981.
- [8] W. Hu. Ringing in the new cosmology: Implications of recent cosmic microwave background experiments. *ANL Physics Division Colloquium*, May 19, 2000.
- [9] Wayne Hu, Douglas Scott, Naoshi Sugiyama, and Martin White. The effect of physical assumptions on the calculation of microwave background anisotropies. *Phys. Rev.*, D52:5498–5515, 1995.

- [10] E. W. Kolb and M. S. Turner. The early universe. Redwood City, USA: Addison-Wesley (1990) 547 p. (Frontiers in physics, 69).
- [11] A. E. Lange et al. First estimations of cosmological parameters from BOOMERANG. 2000. astro-ph/0005004.
- [12] A.R. Liddle and D.H. Lyth. *Cosmological Physics and Large Scale Structure*. Cambridge University Press, Cambridge, UK, 2000.
- [13] Chung-Pei Ma and Edmund Bertschinger. Cosmological perturbation theory in the synchronous and conformal newtonian gauges. *Astrophys. J.*, 455:7–25, 1995.
- [14] P. D. Mauskopf et al. Measurement of a peak in the cosmic microwave background power spectrum from the North American test flight of BOOMERANG. *Astrophys. J.*, 536:L59–L62, 2000.
- [15] A. Melchiorri et al. A measurement of Omega from the North American test flight of BOOMERANG. *Astrophys. J.*, 536:L63–L66, 2000.
- [16] C. W. Misner, K.S. Thorne, and J.A. Wheeler. *Gravitation*. Freeman, New York, 1973.
- [17] Lisa Randall, Marin Soljatic, and Alan H. Guth. Supernatural inflation: Inflation from supersymmetry with no (very) small parameters. *Nucl. Phys.*, B472:377–408, 1996.
- [18] Lisa Randall and Scott Thomas. Solving the cosmological moduli problem with weak scale inflation. *Nucl. Phys.*, B449:229–247, 1995.
- [19] Uros Seljak and Matias Zaldarriaga. A line of sight approach to cosmic microwave background anisotropies. *Astrophys. J.*, 469:437–444, 1996.
- [20] G. F. Smoot. The cosmic background explorer (COBE) results. In *Madrid 1992, Proceedings, Perspectives on high energy physics and cosmology* 136-147.
- [21] M. Tegmark. Cosmological constraints from current CMB and SN 1a data: a brute force 9 parameter analysis. *Astrophys. J.*, 514:L69–L72, 1999.

- [22] M. Tegmark and G. Efstathiou. A method for subtracting foregrounds from multi-frequency cmb sky maps. *MNRAS*, 281:281, 1996.
- [23] Michael S. Turner. Cosmological parameters. *Proceedings of COSMO-98: International Workshop on Particle Physics and the Early Universe*, November 15-20, 1998. These proceedings are to be published.